Applying joint traveltime and waveform inversion to image the Sichuan basin, China

Ziang Li, Jie Zhang, University of Science and Technology of China (USTC)*

Summary

We apply a joint first-arrival traveltime and early-arrival waveform inversion method to image complex near surface structures in Sichuan basin, China. The area includes rugged topography and a large range of velocity variations in the near-surface area. Due to the near surface effects, it is difficult to produce clear reflection images for the deep subsurface. Waveform inversion should allow resolving complex structures. However, it often produces artifacts in the very shallow area due to higher energy close to shot points, and rugged topography also imposes challenge for inversion. Combining with the first-arrival traveltime inversion in a joint fashion, the joint inversion results are more reliable and contain less artifacts. We demonstrate the effectiveness of the joint inversion using synthetics and Sichuan data.

Introduction

Traveltime tomography applies raytracing to compute both the traveltimes and Frechet derivatives (raypaths). While computationally efficient, traveltime tomography is subject to a high-frequency assumption about the data and may not be accurate when the earth's velocity variations are characterized by the same wavelength as in the source wavelet (Luo et al., 1991). Full waveform inversion (FWI) should resolve model velocity details because FWI is based on the waveform theory and should be able to image geologically complex areas (Tarantola, 1984; Sheng et al., 2006). In addition, the model resolution of traveltime tomography is less than waveform inversion. (Gauthier et al., 1986). On the other hand, traveltime tomography constrains very shallow velocities fairly well, while FWI may produce artifacts in the very shallow area due to large variations in amplitudes at very near offset.

In this study, we apply a joint traveltime and waveform inversion method developed by Zhang and Chen (2014) to process a real dataset acquired in Sichuan, China. This dataset is collected to explore potential oil and gas production capability in East Sichuan basin.

The traveltime tomography method applies a graph approach for wavefront raytracing (Zhang and Toksöz, 1998), and waveform inversion employs a finite difference method for wave field simulation (Zhang and Zhang, 2011). The joint inversion is accomplished by using the conjugate gradients method.

Significant topography variations is usually required to handle in FWI, in this study, we concentrate on the influence of rugged topography, because the wave field associated with the rugged topography is very complex, which produces artifacts in waveform inversion.

Geophysical inverse problems are fundamentally non-unique (Aki and Richards, 1980). That means there could be many local minimum solutions for both traveltime tomography and full waveform inversion. However, nonlinear traveltime tomography often has less local minimum solutions than waveform inversion. Joint traveltime and waveform inversion takes a compromise between the first-arrival traveltime inversion and early-arrival waveform inversion and should produce less local minimum solutions than waveform inversion alone (Figure 1). In other words, the joint inversion results should contain less artifacts than waveform inversion results.

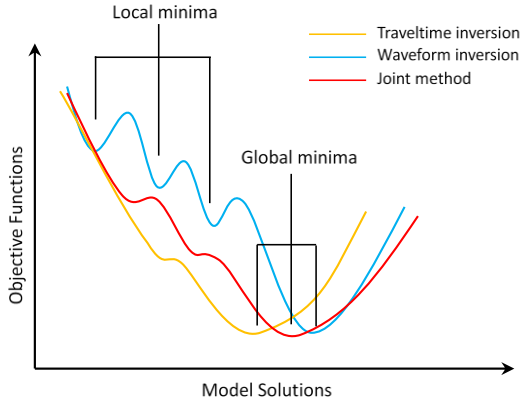

Figure 1: Schematic plot explaining local minima and global minima for three different methods

Joint traveltime and waveform inversion

The objective function of joint traveltime and waveform inversion:

$$\phi(\mathbf{m}) = (1-\omega)\left\|\mathrm{P_o} - \mathrm{P_s}(\mathbf{m})\right\|^2 + \omega\left\|\mathrm{t_o} - \mathrm{t_s}(\mathbf{m})\right\|^2 + \tau\left\|\mathbf{L}(\mathbf{m}-\mathbf{m}_0)\right\|^2$$

Where P_o is observed data, P_s is calculated waveform, t_o is picked traveltime, t_s is synthetic traveltime, $\mathbf{m}$ is the velocity model, $\mathbf{m_0}$ is a priori model. $\mathbf{L}$ is a Laplacian

operator for regularization, ω is a scaling factor between waveform residual and traveltime residual (Zhang and Chen, 2014).

In the objective function, traveltime raypath could help waveform inversion finding solutions quicker by preconditioning the gradient of the objective function (Zhang and Chen, 2014).

Conjugate gradient algorithm is applied to solve the joint inversion problem. During the inversion process, selection of a weighting factor ω between waveform misfit and traveltime misfit is an important issue. If ω is too high, the joint inversion will yield a smoothed and low resolution model close to the first-arrival traveltime tomography. If ω is too small, the joint inversion cannot constrain the near-surface velocity well (Jiang and Zhang, 2015).

Synthetic test

We design a numerical experiment to test joint inversion. We build a true model according to a geological model of Chuandong Oil Field. The model is shown in Figure 2a, which includes high-velocity contrasts, rugged topography and a low velocity object. Figure 2b shows that the result of first-arrival traveltime tomography seems to be reasonable. But the low velocity object cannot be imaged. To image the low velocity object and get a more accurate velocity model, we consider to do the waveform inversion with the Ricker wavelet at frequency from 5 Hz to 9 Hz because imaging different sizes of structures requires different frequencies of wave field information. For example, we use the result of the traveltime tomography as an initial model and use 5 Hz Ricker wavelet to do the waveform inversion, then we use the result of 5 Hz waveform inversion as the initial model and use the 6 Hz Ricker wavelet to do the waveform inversion. Finally we can get the result of the waveform inversion by such multiscale strategy. Figure 2c shows the result from waveform inversion after 50 iterations. The result of joint inversion after 20 iterations is shown in Figure 2d, not only the iterations of joint inversion is reduced, but also the joint method provides a reliable velocity model.

Compared with the traveltime tomography, FWI could establish the low velocity zone, but the layers under the rugged topography are not reliable because the velocity is too high near the V-shaped surface (marked by the black circle). Joint traveltime and waveform inversion keeps most of the features in FWI results, but lowers the near surface velocities so that inverts the velocity model more accurate.

a) True model

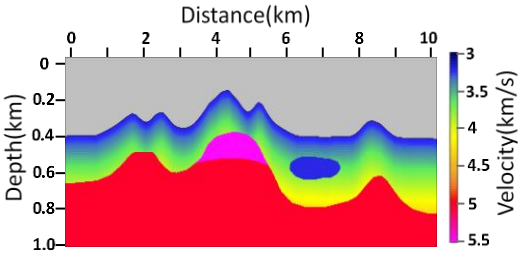

b) Traveltime tomography

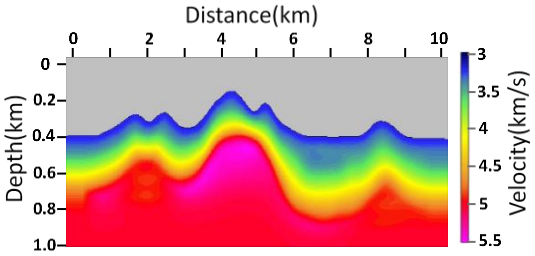

c) Waveform inversion

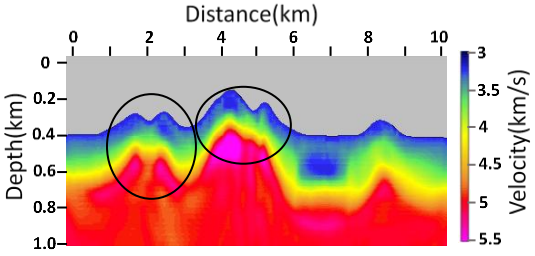

d) Joint inversion

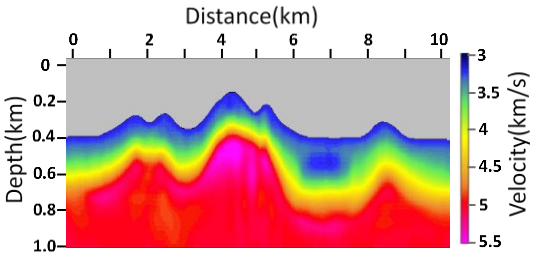

Figure 2: Synthetic experiment: a) True model; b) Traveltime tomography result; c) Waveform inversion result; d) Joint traveltime and waveform inversion result.

Sichuan data example

We process a real 2D dataset from Sichuan, China with the above method. The data consists 194 shots with shot spacing of 40 m and receiver spacing of 20 m. The area includes rugged topography and a large range of velocity variations in the near-surface area.

The initial model is analytically created by picking refraction turning points from the first arrival traveltimes (Figure 3a). The first arrival traveltime tomography generates a velocity solution shown in Figure 3b. Following the first arrival picks on the waveform data, we keep a window of 150 ms for early arrivals and mute the remaining data for waveform inversion. Figure 3c shows the early-arrival waveform inversion result after 20 iterations. The joint inversion result is shown in Figure 3d, it just needs 12 iterations to obtain the final result with satisfied misfit.

Waveform inversion presents more velocity details in the model than the traveltime tomographic solution. But waveform inversion also presents high velocity artifacts (marked by the red circle) near the V-shaped surface. In the result of joint traveltime and waveform inversion. The top near surface area shows similar velocities to the traveltime tomography results. In this area, waveform inversion produces artifacts of higher velocity, joint inversion overcomes the influence of the rugged topography and lowers the velocity due to the constraints of the first-arrival traveltime.

a) Initial model

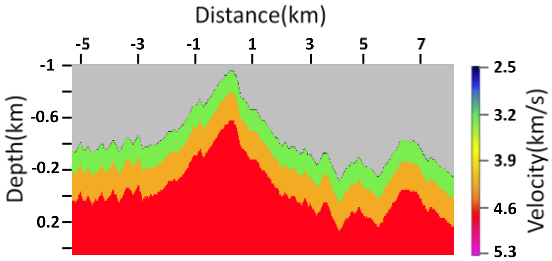

b) Traveltime tomography

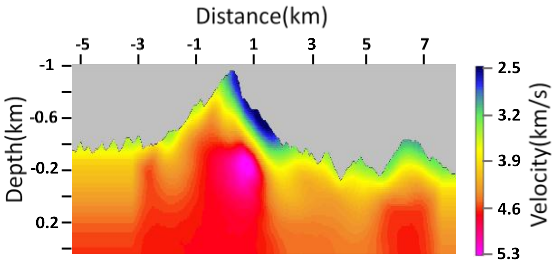

c) Waveform inversion

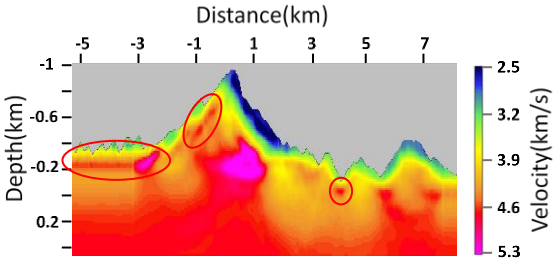

d) Joint inversion

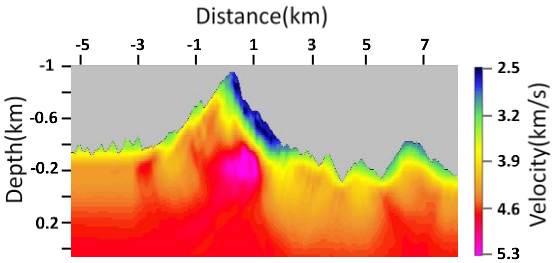

Figure 3: Sichuan data experiment: a) Initial velocity model; b) Traveltime tomography solution; c) Waveform inversion solution; d) Joint traveltime and waveform inversion solution.

Figure 4a shows the data misfit of waveform inversion and joint inversion. For waveform inversion, data misfit means just the waveform misfit, but for joint inversion, data misfit means the total misfit of waveform and traveltime. Therefore, the data misfit of the joint inversion is higher than that of waveform inversion because the joint inversion needs to fit both waveform and traveltime, but the joint inversion converges faster than the waveform inversion.

Figure 4b shows the waveform data misfit of waveform inversion and joint inversion. The joint inversion helps significantly speeding up waveform inversion and obtains the final result with more satisfied waveform misfit.

a) Data misfit

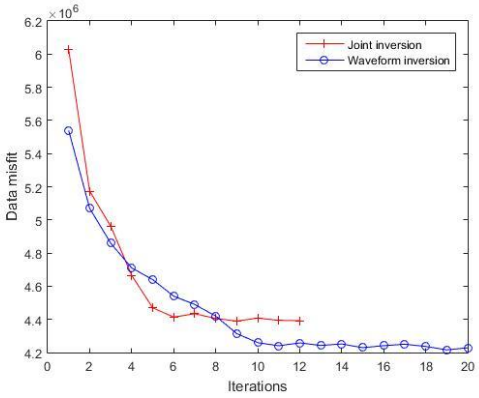

b) Waveform misfit

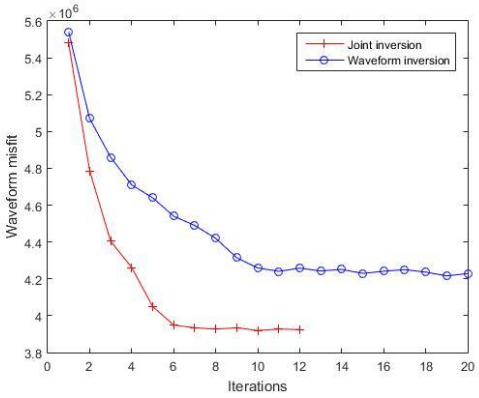

Figure 4: Misfit comparison: a) Data misfit of joint inversion (red) and waveform inversion (blue); b) Waveform misfit of joint inversion (red) and waveform inversion (blue).

Furthermore, we compare the waveform match between waveform inversion and joint inversion. Figure 5a displays one of the shot gathers and compares data (black) with the corresponding synthetic waveform (red) after 20 iterations of waveform inversion. The overall waveform match seems to be reasonable, but the synthetic waveform does not actually match the first arrival at the large offset.

Figure 5b shows the overlay of a shot gather (black) with synthetic waveform (red) after 12 iterations of joint inversion. The waveform match is improved especially at the large offset and the first arrival traveltime are also better matched.

a) Waveform match from waveform inversion alone

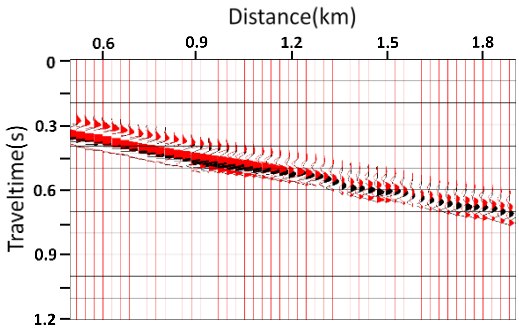

b) Waveform match from the joint inversion

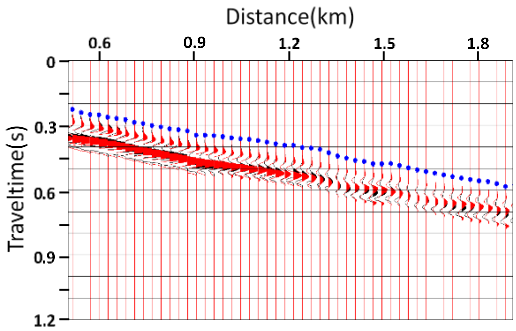

Figure 5: Waveform match: a) synthetics (red) and input data (black) after 20 iterations from waveform inversion; b) synthetics (red) and input data (black) after 12 iterations from the joint inversion (Blue line represents the first arrival picks.).

Conclusions

This study shows that joint traveltime and waveform inversion can produce a reasonable solution for areas with rugged topography and a large range of velocity variations in the near-surface area. We apply joint method to synthetics and Sichuan data. The results show the joint inversion are more reliable than traveltime tomography or waveform inversion alone. Nevertheless, non-uniqueness is a fundamental issue in FWI. Joint traveltime and waveform inversion may not solve this problems entirely, but joint method should improve the solution due to the constraints of both traveltime and waveform.

Acknowledgments

We appreciate the support from GeoTomo, allowing us to use TomoPlus software package to finish this work.

EDITED REFERENCES

Note: This reference list is a copyedited version of the reference list submitted by the author. Reference lists for the 2016 SEG Technical Program Expanded Abstracts have been copyedited so that references provided with the online metadata for each paper will achieve a high degree of linking to cited sources that appear on the Web.

REFERENCES

Aki, K., and P. G. Richards, 2002, Quantitative seismology, 2nd ed.: University Science Books.

Gauthier, O., J. Virieux, and A. Tarantola, 1986, Twodimensional nonlinear inversion of seismic waveforms — Numerical results: Geophysics, **51**, 1387–1403, http://dx.doi.org/10.1190/1.1442188.

Jiang, W., and J. Zhang, 2015, Imaging complex near-surface land area with joint traveltime and waveform inversion: 85th Annual International Meeting, SEG, Expanded Abstracts, 142–145, http://dx.doi.org/10.1190/segam2015-5863831.1.

Luo, Y., and G. T. Schuster, 1991, Wave-equation traveltime inversion: Geophysics, **56**,. 5, 645–653, http://dx.doi.org/10.1190/1.1443081.

Sheng, P., 2006, Introduction to wave scattering, localization and mesoscopic phenomena: Springer Science & Business Media.

Tarantola, A., 1984, Inversion of seismic reflection data in the acoustic approximation: Geophysics, **49**, 1259–1266, http://dx.doi.org/10.1190/1.1441754.

Zhang, J., and J. Chen, 2014, Joint seismic traveltime and waveform inversion for near surface imaging: 84th Annual International Meeting, SEG, Expanded Abstracts, 934–937.

Zhang, J., and M. N. Toksöz, 1998, Nonlinear Refraction Traveltime Tomography: Geophysics, **63**, 1726–1737, http://dx.doi.org/10.1190/1.1444468.

Zhang, W., and J. Zhang, 2011, Full waveform tomography with consideration for large topography variations: 81th Annual International Meeting, SEG, Expanded Abstracts, 2539–2542, http://dx.doi.org/10.1190/1.3627719.